Available online at www.sciencedirect.com
ScienceDirect
Journal of Non-Crystalline Solids 352 (2006) 3391–3397
JOURNAL OF NON-CRYSTALLINE SOLIDS
www.elsevier.com/locate/jnoncrysol

Crystallization of a niobium phosphate glass

L. Ghussn [a], M.O. Prado [b], D.O. Russo [b], J.R. Martinelli [a,*]

[a] *Instituto de Pesquisas Energéticas e Nucleares, Av. Prof Lineu Prestes, 2.242, Cidade Universitária, São Paulo/SP, CEP 05508-000, Brazil*
[b] *Centro Atómico Bariloche, Av. Bustillo, Km 9.5, San Carlos de Bariloche, RN, CP 8400, Argentina*

Available online 1 August 2006

Abstract

Niobium phosphate glasses with composition $37P_2O_5 \cdot 23K_2O \cdot 40Nb_2O_5$ are stable in relation to crystallization during the heating process, exhibit a low critical cooling rate, and are potentially good for nuclear wasteforms. The crystallization of these glasses was evaluated by optical microscopy after proper heat treatments, showing that surface crystallization is the main process occurring during the heat treatment. Two main crystalline phases were observed. These crystalline phases were KNb_3O_8 and $K_3NbP_2O_9$. Surface crystal growth rates were measured in the temperature range of 806–972 °C ($T_g = 683$ °C) for both crystalline phases. Apparent crystallization enthalpies were determined through the Arrhenius plots of lnU vs. $1/T$. The enthalpies are 496 kJ/mol and 513 kJ/mol for each crystalline phase, respectively. The surface density of nucleation sites (N_s) on 3 μm diamond paste polished surfaces is $(2.4 \pm 0.7) \times 10^8$ nuclei/m^2 for one crystalline phase and $(9.8 \pm 0.8) \times 10^9$ nuclei/m^2 for the other crystalline phase, when revealed at 838 °C/17.5 h, and these values show a slight variation depending on the time and the temperature. At the tested temperatures, only one crystal phase appeared inside the volume, and a volume density of nucleation sites $N_v = 5 \times 10^6$ nuclei/m^3 was measured.

PACS: P147; C290; C2865

Keywords: Crystallization; Nucleation; Phosphates

1. Introduction

There has always been a concern about the final destination of nuclear wastes since the beginning of the use of the nuclear energy for power generation. When leakages of nuclear wastes were detected on storage tanks, research efforts were employed to reach for a solution to prevent the contamination of the environment with nuclear wastes, and different solutions were proposed. One of them was the immobilization of nuclear waste in glass matrices. As the industry was prepared to easily produce some chemical resistant glasses, borosilicate glasses were chosen as the preliminary, and hopefully, the final solution. However, the chemical composition of nuclear waste is not unique and there is not only one glass composition, or even, a narrow range of glass composition that could be used for all nuclear wastes. For example, wastes containing chromium, phosphorous, etc. can cause phase separation, or even crystallization in borosilicate glasses.

Phosphate glasses could deteriorate in humid environments, and that was an important issue. When iron was added to the composition of phosphate glasses, the chemical durability improved, creating a new area of research.

Lead iron phosphate glasses (LIPG) had been previously proposed to be used as a matrix for the immobilization of nuclear wastes [1]. LIPG can be obtained at lower melting temperatures (usually ~1100 °C) when compared to borosilicate glasses. Concerning the chemical durability, the dissolution rate of LIPG could be 1000 times lower than the ones for borosilicate glasses when samples are leached at 90 °C in aqueous solution with pH in the range of

* Corresponding author. Tel.: +55 11 38169346.
E-mail address: jroberto@ipen.br (J.R. Martinelli).

0022-3093/$ - see front matter © 2006 Elsevier B.V. All rights reserved.
doi:10.1016/j.jnoncrysol.2006.02.105

5–9 [2]. However, LIPG are susceptible to crystallization if glass blocks with more than 5 cm in diameter and 10 cm high are prepared. This effect can be disruptive to the main characteristics required for wasteforms. At a previous work we proposed the replacement of iron oxide by niobium oxide, since large amounts of niobium are available in Brazil, the properties of the material would be less susceptible to valence changes, and the corrosion resistance of niobium phosphate glasses has been proved to be better than the one for iron phosphate glasses. These glasses could be prepared in electrical furnaces, induction furnaces, and in microwave ovens.

Sintered barium lead niobium phosphate glasses were considered as potential candidates for the immobilization of nuclear wastes [3], however crystallization was observed after sintering for periods of time longer than 12 h. Promising results were also reported for niobium phosphate glasses without barium and lead. Niobium phosphate glasses $37P_2O_5$–$23K_2O$–$40Nb_2O_5$ show dissolution rates of 10^{-6} g/cm^2/day, when leached at 90 °C in aqueous solution. This value is in the range of values previously reported for lead free iron phosphate glasses [3]. However, crystalline phases were formed during the sintering process. There might be interference in the physicochemical properties of the material if crystallization occurs during glass melting and forming, or during glass powder sintering.

If wastes are incorporated to the matrix glass by sintering a powder mixture, the large specific surface area of the glass will represent a large density of nucleation sites for crystallization; nucleation sites are provided by the surface area. If the glass is poured into moulds, surface crystallization will occur only at the glass-mould interface; however homogeneous crystallization might be responsible for the crystallization in the volume.

Since scarce information is available on crystallization of niobium phosphate glasses, the occurrence of crystallization of the glass matrix was investigated in this work. The crystal growth of two different crystalline phases was measured and the apparent crystallization enthalpy was determined considering an Arrhenius behavior. These values were compared with values previously reported in the literature for other phosphate and silicate glasses.

2. Experimental methods

2.1. Glass preparation

A niobium phosphate glass was obtained by melting mixtures of inorganic precursors (Reagent Grade) in an electrical furnace at 1350 °C for 1 h in alumina crucibles. The glass composition is $37P_2O_5$–$23K_2O$–$40Nb_2O_5$ in mol% (named in the present work as Nb40). The raw materials were Nb_2O_5 (supplied by the Companhia Brasileira de Metalurgia e Mineração, CBMM, Brazil), $NH_4H_2PO_4$ (Merk) and KOH (Cicarelli). The liquid was cast in a stainless steel mold and annealed at 697 °C.

2.2. Characterization

The density of each glass was measured by the Archimed's method. X-ray diffraction analysis (XRD) was performed in the 2θ angle range of 3.5–90° (Philips, model PW1700), by using the Cu Kα radiation. Differential thermal analysis (DTA) was performed for powder glass samples (Netzsch, model STA 409) at 10 °C/min, in a dynamic air flow, from room temperature to 1320 °C. The DTA was also recorded during the cooling cycle at 10 °C/min, and the sample was re-heated again to 1320 °C.

The thermal stability (resistance to crystallization on heating) was evaluated considering the parameter proposed by Hrubý (K_H), which can be determined from the DTA curve, according to the following equation:

$$K_H = \frac{T_c^h - T_g}{T_m^* - T_c^h}, \quad (1)$$

where T_c^h is the onset of the crystallization peak, T_g is the glass transition temperature, T_m^* is the melting temperature.

According to Hrubý and Houserova [4], the more stable the glass is, the higher K_H will get (the glass will be less susceptible to crystallization during the cooling).

Micrographs were taken by using an optical microscope and a scanning electron microscope (Philips model XL30) to observe the glass surfaces after different heat treatments and to determine the crystal sizes and counts.

2.3. Surface crystallization

The crystal growth rate was determined from the grain size as a direct functional relationship between time and temperature of heat treatment and by calculating the slope of a plot of crystal size vs. time. The same procedure was applied at different temperatures. The crystal density was determined by the number of crystals counted in a given surface area. Since two different kinds of crystals (distinguished by their size) were observed on the surface, this procedure was performed for each type of crystal.

An optical microscope was used to determine the number and the crystal size on the sample surfaces. Crystal growth rates were determined by measuring the largest crystal size on the surface. Surface density of nucleation sites were determined by counting the number of developed crystals in random optical fields of a known area.

For the small crystals, the nucleation density was determined by counting the number of crystals per surface area by analyzing 10 different micrographs. The same procedure was used for the large crystals, except that a larger number of micrographs were used because the number of crystals per surface area was smaller. The size of the crystal was assumed to be the largest linear dimension and the crystal growth rate was determined considering half of that value as a direct functional relationship of the time of heat treatment.

Table 1
Temperatures and times used to nucleate surface crystalline sites on Nb40 glasses

Temperature (°C)	Time (min)
806	900–3600
838	360–3120
871	125–215
905	7–102
937	5–25
972	2–7

Glass samples $2 \times 2 \times 1\ mm^3$ were polished to 1000 grit with SiC paper, and finally polished to 0.3 μm with diamond powder cloth and heat treated at various temperatures and times. Table 1 presents the experimental parameters used for the nucleation study.

To avoid residual contamination from polishing which could induce crystallization in the glass, samples were washed in distilled water with ultrasound three times during 3 min each turn, changing the water, and letting them to dry in hot air. The crystalline phases were observed on the surface of these samples. The surface density of nucleation sites (N_s) was determined by developing the crystals at a given temperature T, counting the number of crystals in a known glass surface area. N_s was measured as a function of time and temperature (see Section 3.2).

2.4. Volume crystallization

Glass samples $1.5 \times 1.7 \times 0.7\ cm^3$ were heat treated at 806 °C for different times (24, 48, 96, 120 h) to induce the nucleation and afterwards at 838 °C/24 h for growing. This procedure was necessary to allow the counting of the sites. Since surface crystallization occurred, a crystalline layer arose around the samples, but they were large enough to remain glassy inside.

To determine the volume density of nucleation sites, samples were imbedded in a resin and sliced to facilitate the observation inside the bulk by using a microscope. Since there was the occurrence of only few crystals in the whole sample volume after heat treatment, N_v values were determined as the quotient between the total number of crystals found in all the equivalent samples and their total volume. Five samples of the glass were analyzed to determine the volume density of nucleation sites (N_v).

3. Results

3.1. Differential thermal analyses

Fig. 1 shows the DTA curve for a NB40 glass.

An endothermic step is observed at 683 ± 3 °C. An exothermic peak with the onset at 924 ± 4 °C, maximum at 936 ± 3 °C, and ending at 947 ± 4 °C, and an endothermic peak at 1178 ± 2 °C are also observed.

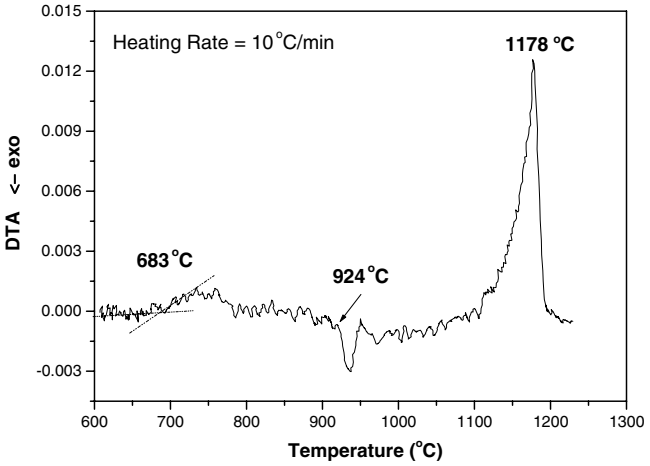

Fig. 1. DTA curve for a monolithic Nb40 glass.

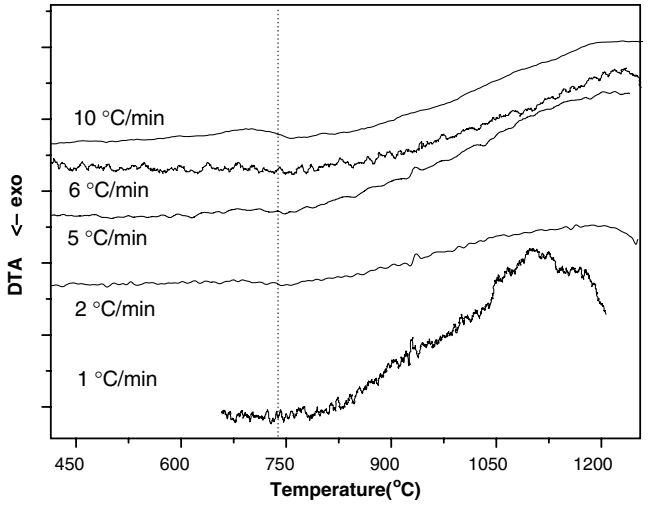

Fig. 2. DTA curves with different cooling rates for Nb40 glasses.

Fig. 2 shows the DTA curves for Nb40 glass samples cooled at different cooling rates during the analyses. From these data the critical cooling rate q_{cr} was determined.

Differential thermal analyses were also performed for powder glass samples with different particle size distributions. Fig. 3 shows the DTA curves obtained for three different particle size distributions shown in Fig. 4 for the NB40 glass.

3.2. Nucleation and crystallization

Nb40 glass samples were heat treated in the temperature range of 800–980 °C, for times in the range of 2–3600 min. Particularly, no crystal formation was observed on the glass surface after heat treating at 791 °C/72.5 h.

After the heat treatment the surfaces of the samples were observed by using optical and scanning electron microscopes. Fig. 5 shows the scanning electron micrograph of the surface of a glass sample after the heat treatment for

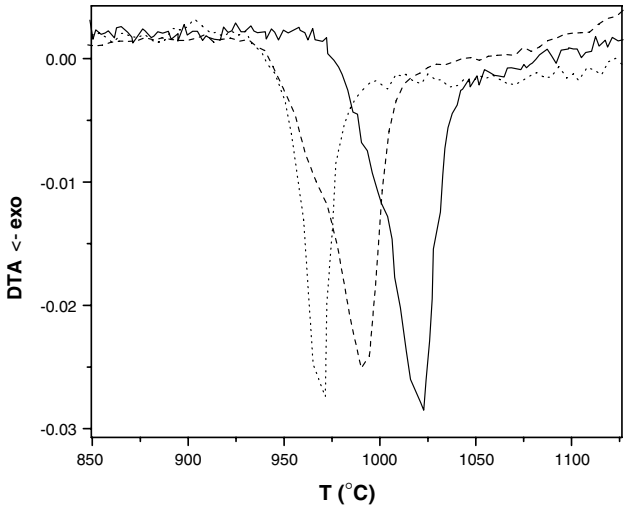

Fig. 3. DTA curves (850–1150 °C) for glass powders with different particle size distributions; (. . .). Fine particles; (- - -) fine + coarse particles; (—) coarse particles. As the particles get coarser, T_c is displaced to higher temperatures.

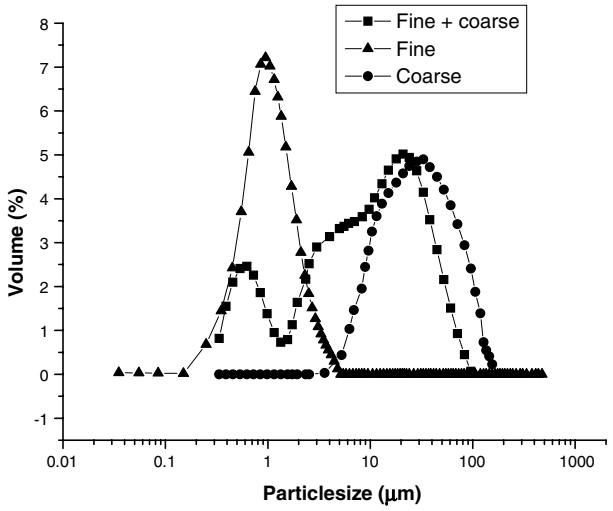

Fig. 4. Corresponding particle size distribution for the NB40 glass.

crystallization. Two different crystalline phases (named in this work as α1 and α2), and distinguished themselves by the size of the crystals, are observed on the surface.

The X-ray diffraction pattern shown in Fig. 6 is for the Nb40 glass after heat treatment at 972 °C/4 h.

The glass density determined by the Archimedes principle is 3.42 g/cm^3.

Fig. 7 shows the SEM micrograph of the glass surface, after heat treatment at 838 °C/17 h.

The crystal growth was determined for different temperatures. Fig. 8 shows the crystal growth at 972 °C for the large crystals (α2).

Table 2 presents the crystal growth rate and the density of nucleation sites for two different crystalline phases found on the surface of the Nb40 glass.

Table 3 presents some data of surface nuclei density reported elsewhere corresponding to different glass systems, for comparison with our glass. Details concerning the reported values can be found in Ref. [5].

Concerning the volume nucleation, only after 120 h at 806 °C and 24 h at 838 °C volume crystallization could be observed. No crystals were observed after heat treatments at 806 °C/24–96 h followed by 838 °C/24 h, which is evi-

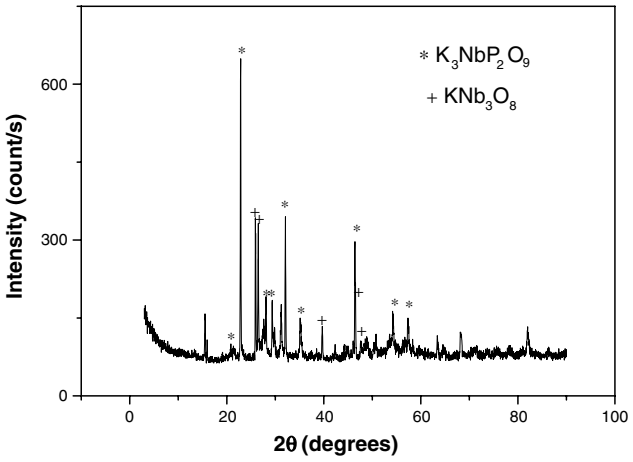

Fig. 6. X-ray diffraction pattern for a Nb40 glass crystallized at 972 °C/4 h.

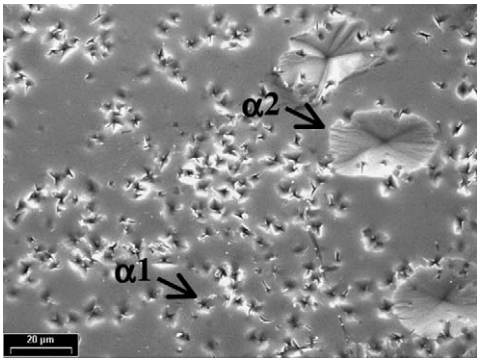

Fig. 5. Micrograph of a glass surface (Nb40-type glass) after heat treating at 838 °C/17 h.

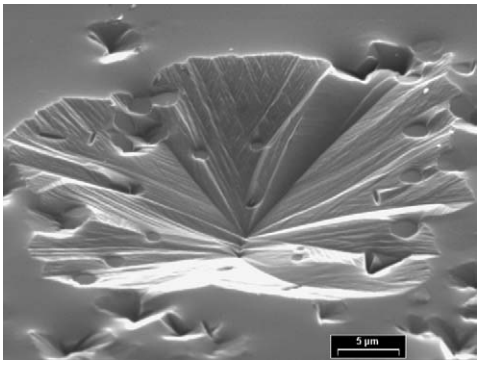

Fig. 7. SEM micrograph of a glass surface (Nb40-type glass). Small and large crystals can be observed, besides the glass matrix.

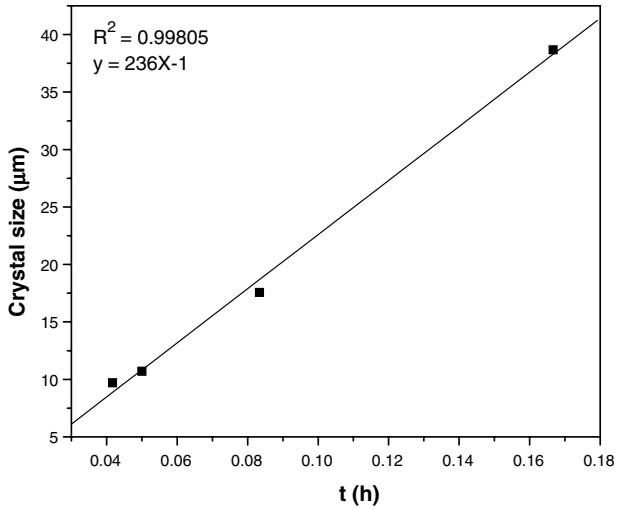

Fig. 8. Crystal size as a function of time (t) for a constant temperature (972 °C).

dence that the nucleation at 838 °C can be distinguished at this temperature. Therefore, five 1.82 cm^3 samples were heat treated during 120 h at 806 °C and during 24 h at 838 °C and 33, 3, 6, zero and zero crystals were observed on each individual sample. The nucleation site density was calculated considering the ratio between the number of crystals and the volume of the sample, and the average nucleation site density is 5×10^6 nuclei/m^3.

The apparent enthalpy for crystallization was determined considering the Arrhenius behavior as shown in Fig. 9, where the growth rate is plotted against the reciprocal of the absolute temperature.

For the Nb40 glass the activation energies for crystallization of phases α1 and α2 were determined to be 496 ± 7 kJ/mol and 513 ± 14 kJ/mol, respectively.

4. Discussion

4.1. Hrubý parameter and critical cooling rate

The endothermic step observed at 683 ± 3 °C in the DTA curve of Fig. 1 might happen due to the glass transition. The exothermic peak with the onset at 924 ± 4 °C, maximum at 936 ± 3 °C, and ending at 947 ± 4 °C is due to a crystallization process. The endothermic peak at 1178 ± 2 °C is due to the melting of that crystalline phase.

Table 3
Density of nucleation sites (N_s) for different materials

System	N_s (nuclei/m^2)	Reference
$Li_2O \cdot 2SiO_2$ (lithium disilicate)	6×10^{21}	[5]
$CaO \cdot Al_2O_3 \cdot 2SiO_2$(anorthite)	5×10^{16}	[5]
$PbO \cdot SiO_2$	2×10^{13}	[5]
Crystoballite (plain glass)	2×10^9	[6]

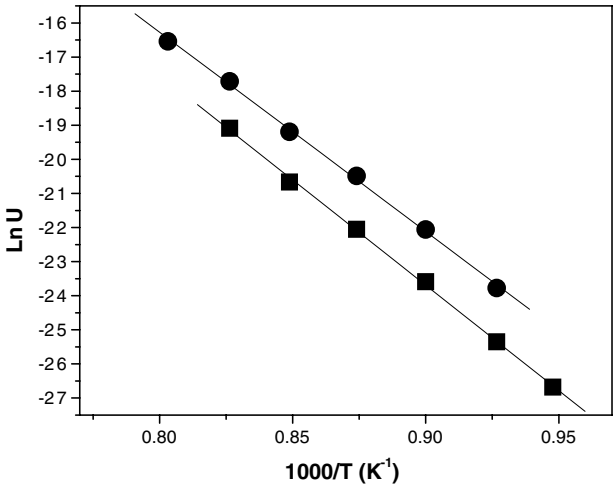

Fig. 9. Crystal growth rate as a function of reverse temperature for the following crystalline phases: (■)α1 and (●) α2.

For the Nb40 glass K_H is 0.95 ± 0.04. This value is relatively high when compared to reported values for silicate glasses [7] in the range of 0.14 ± 0.03 to 0.68 ± 0.05. Therefore the Nb40 glass is very thermally stable.

No exothermic peaks that could be related to crystallization process were observed for cooling rates higher than 2 °C/min in Fig. 2. Although the same was true for samples cooled at 1 °C/min, some white spots were observed on the surface of the sample in the crucible after cooling, but the bulk was still transparent indicating that surface crystallization occurred. Since a discrete crystallization process occurs at 1 °C/min, this cooling rate is assumed to be critical. This cooling rate is relatively low when compared to critical cooling rates reported for the $40LiO_2$–$60SiO_2$ glass [7]. The value reported is 24 ± 6 °C/min. Therefore the Nb40 glass composition can easily be prepared if cooling rates higher than 1 °C/min are used.

It is important to notice that when cooling large glass blocks as the ones found in an industrial scale, the cooling

Table 2
Crystal growth rate (v) and surface density of nucleation sites (N_s) for phases α1 and α2 at different heat treatments

Heat treatment	$v\alpha_1$ (μm/h)	$v\alpha_2$ (μm/h)	$N_s\alpha_1$ (nuclei/m^2)	$N_s\alpha_2$ (nuclei/m^2)
806 °C/24 h	0.035 ± 0.002	0.171 ± 0.001	$(1.3 \pm 0.4) \times 10^{10}$	$(8.3 \pm 0.8) \times 10^7$
838 °C/12 h	0.205 ± 0.003	0.949 ± 0.003	$(3.9 \pm 1.2) \times 10^{10}$	$(2.4 \pm 0.5) \times 10^8$
871 °C/2 h	0.95 ± 0.08	4.56 ± 0.13	$(6.4 \pm 0.9) \times 10^{10}$	$(2.9 \pm 0.6) \times 10^8$
905 °C/35 min	3.8 ± 0.3	16.6 ± 0.9	$(8.4 \pm 1.8) \times 10^{10}$	$(6.7 \pm 2.2) \times 10^8$
937 °C/10 min	18.4 ± 0.9	73 ± 2	NA[a]	NA[a]
972 °C/3 min	NA[a]	235 ± 25	NA[a]	NA[a]

[a] Not available.

rate inside the block is always lower than the one at the surface. For a borosilicate glass block 30 cm in diameter and 74 cm high, it takes 3 h to reach 800 °C inside the block from the starting temperature of 1100 °C [2]. That means an approximated cooling rate of 1.7 °C/min. This value is higher than the one determined for the Nb40 in this work, so the Nb40 glass would not have appreciable bulk crystallization in that situation.

4.2. DTA analysis with different particle size distributions

Considering that crystals grow from the surface during the heating process, samples with larger specific surface (smaller particle size) exhibit lower crystallization temperature. If we assume that there is a surface density of nucleation sites N_s, as the specific surface of the powder increases, the number of nucleation sites in the sample will also increase.

Otherwise if only homogeneous nucleation takes place, the specific surface will not affect the temperature of the crystallization peak in the DTA curves of different particle size distributions.

Smaller particles display lower crystallization temperatures which confirm the presence of surface crystallization.

4.3. Crystallization

Two crystalline phases observed in Fig. 5 were identified by X-ray diffraction: KNb_3O_8 (JCPDS 28-0788) and $K_3NbP_2O_9$ (JCPDS 48-0863).

Since the number of crystals is low after heat treatments at temperatures lower than 972 °C, X-ray diffraction patterns were obtained, in this case, from powder samples so a larger surface area would provide an amount of crystalline phases above the minimum detection limit of the X-ray diffraction analysis. As an example, a powder sample was heat treated at 905 °C/3 h, grounded, and heat treated again at the same temperature and time. This procedure was repeated three times before getting the X-ray diffraction pattern, so the diffraction peaks related to crystalline phases could be resolved. The identified crystalline phases were the same ones previously observed for the heat treatments performed at higher temperatures. The same procedure was done for a sample heat treated at 1030 °C, and the same crystalline phases were identified.

Since the crystalline phase density is larger than the corresponding amorphous phase density, the crystal growth will occur from the surface to the bulk of the sample. This effect can be easily seen on the SEM micrograph presented in Fig. 7.

The presence of tiny crystals on the surface of the large crystal, with the same apparent morphology as the α1 crystals, is also observed in Fig. 7. It is not possible at the moment to assure that these crystals are α1-type crystals, however, if they are, there are two possible reasons: (1) since one of the phases does not have phosphorous in its structure (as demonstrated by the XRD), one region will be depleted of phosphorous atoms and the other region will be P-rich, and both kind of crystalline phases will be found in the same region; (2) since the crystalline phases have different growth rates, the α2 crystal will involve the α1 crystal, considering that both nuclei are close enough during the nucleation process.

Besides that, regions with circular shapes can also be observed on the surface of the α2 crystals, which could be assigned to a third crystalline phase, not identified by XRD, or a residual glass phase. Further work is required to confirm this observation, even with glasses with different amounts of niobium.

The surface density of nucleation sites (N_s) increases as the temperature is raised, and for a 100 °C rise, the number of nuclei increases almost one order of magnitude. However, there is an experimental limit to perform that measurement. For temperatures higher than 905 °C samples become soft and the original flat surface of the glass sample becomes rounded, making the measurement of the surface area difficult because of the limited depth of field of the optical microscope. In this case, since the N_s measurement was not accurate, they were discarded.

For the Nb40 glass, the maximum N_s value is 8×10^{10} nuclei/m^2, considering both crystalline phases. This value is about three times higher than the value reported for plain glasses taking into account just a single phase and two orders of magnitude lower when compared to the value reported for lead silicate glasses.

Metcalfe and Donald [6] reported that the apparent enthalpy for crystallization of two different crystalline phases in sodium iron aluminum phosphate glasses were 363 kJ/mol and 385 kJ/mol, respectively. Enthalpy values reported for silicate glasses [8] are 110 kJ/mol for cristoballite, 115 kJ/mol for β-wollastonite and 220 kJ/mol for devitrite. The enthalpy values determined for the Nb40 glasses ($E\alpha1 = 496 \pm 7$ kJ/mol and $E\alpha2 = 513 \pm 14$ kJ/mol) are higher than the ones reported by Metcalfe and Donald [6]. Therefore, it is assumed that the resistance to crystallization of Nb40 glasses should be higher than the one for iron phosphate glasses previously investigated.

5. Conclusions

A glass with composition $37P_2O_5$–$23K_2O$–$40Nb_2O_5$ in mol% was found to be thermally stable in relation to crystallization during heating: it shows a Hrubý parameter equal to 0.95, which is larger than the ones reported for some known silicate glasses. This is an important characteristic in case the material is considered for the immobilization of nuclear wastes. The critical cooling rate, by cooling from the melt in alumina crucibles, was determined to be 1 °C/min. Therefore, large glass blocks could be obtained without volume crystallization. However, this glass presents surface crystallization if exposed to temperatures above 792 °C. Two crystalline phases, KNb_3O_8 and $K_3NbP_2O_9$ were identified. The apparent enthalpies for crystallization are 496 ± 7 and 513 ± 14 kJ/mol.

Acknowledgements

L. Ghussn thanks CNPq and CAPES – Brazil for the scholarship. Companhia Brasileira de Metalurgia e Mineração (CBMM) is acknowledged for supplying Nb_2O_5. A.M. Sanfilipo and A.D. Heredia are acknowledged for helping with the sample metallographic preparation, and A.S. Prastalo for the mold fabrication. The authors also thank D. Rodriguez for his contribution to the DTA analyses. This work was supported by the International Atomic Energy Agency.

References

[1] B.C. Sales, L.A. Boatner, Science 226 (1984) 45.
[2] W. Lutze, R.C. Ewing, Radioactive Waste Forms for the Future, North-Holland Physics Publishing, Amsterdam, 1988.
[3] L. Ghussn, J.R. Martinelli, J. Mater. Sci 39 (2004) 371.
[4] A. Hrubý, J. Houserova, Czech. J. Phys. 22 (1972) 1187.
[5] M.L.F. Nascimento, PhD thesis, Universidade de São Carlos, São Carlos, 2004.
[6] B.L. Metcalfe, I.W. Donald, Thermal properties and crystallization kinetics of a sodium aluminophosphate based glass, in: Presented at the Annual Meeting of the International Commission on Glass/VI Brazilian Symposium on Glass and Related Materials/II International Symposium on Non-Crystalline Solids/V Latin American Technical Symposium on Glass, Campos do Jordão, Brazil, 15–19 September, 2003.
[7] A.A. Cabral, A.A.D. Cardoso, E.D. Zanotto, J. Non-Cryst. Solids 320 (2003) 1.
[8] J. Deubener, R. Bruckner, H. Hessenkemper, Glastech. Ber. 65 (1992) 256.